ELSEVIER

Thermochimica Acta 352–353 (2000) 127–132

thermochimica acta

www.elsevier.com/locate/tca

Thermal and IR properties of Mg(II) complexes with heterocyclic ligands

S.C. Mojumdar[a,*], M. Melník[b], E. Jóna[c]

[a]*Institute of Inorganic Chemistry, Slovak Academy of Sciences, Dubravska Cesta 9, SK-84236 Bratislava, Slovak Republic*
[b]*Department of Inorganic Chemistry, Slovak Technical University, SK-81237 Bratislava, Slovak Republic*
[c]*Department of Chemistry, University of Trenčin, SK-02032 Púchov, Slovak Republic*

Received 2 June 1999; received in revised form 15 August 1999; accepted 6 September 1999

Abstract

Thermogravimetry (TG), differential thermal analysis (DTA) and other analytical methods have been applied to the investigation of the thermal behavior and structure of the compounds $Mg(pc)(na)_2 \cdot 2H_2O$ (**I**), $Mg(pc)(Et_2na)_2 \cdot 3H_2O$ (**II**), $Mg(pc)(mpc)_2 \cdot H_2O$ (**III**) and $Mg(pc)(ron) \cdot 2H_2O$ (**IV**), where pc=2,6-pyridindicarboxylate, na=nicotinamide, Et_2na=*N*,*N*-diethylnicotinamide, mpc=methyl-3-pyridyl carbamate and ron=3-pyridylcarbinol (ronicol). Thermal decomposition of these compounds are multi-stage processes. The composition of the complexes and the solid state intermediate and resultant products of thermolysis had been identified by means of elemental analysis and complexometric titration. The possible scheme of destruction of the complexes is suggested. Heating the compounds first results in a release of water molecules. In complexes **I**, **II** and **IV** the loss of the molecular ligands (na, Et_2na and ron) occur (on the TG curves) in one step (−2na, −2Et_2na and −ron) and in complex **III** in two steps (−mpc, −mpc). The final product of the thermal decomposition was MgO. The thermal stability of the complexes can be ordered in the sequence: **II<III<I<IV**. Et_2na, na, and ron were coordinated to Mg(II) through the nitrogen atom of the respective heterocyclic ring. IR data suggest to a unidentate coordination of carboxylates to Mg(II) in complexes **I–IV**. © 2000 Elsevier Science B.V. All rights reserved.

Keywords: TG; DTA; IR spectra; Heterocyclic compounds; Mg(II) complexes

1. Introduction

It is well documented that heterocyclic compounds play a significant role in many biological systems, especially N-donor ligand systems being a component of several vitamins and drugs [1,2]. It is not surprising, therefore, that many authors have investigated heterocyclic compounds and also examined them as ligands in coordination compounds of several central atoms [3–14]. In order to enhance understanding of drug–metal ion interactions, we have been studying the thermal properties of Mg(II) complexes with 2,6-pyridindicarboxylic acid (pch) and Et_2na, na, mpc or ron, which are known as important components of biological systems.

The reveal of the relationship between the structure and thermolysis of metal carboxylate complexes, the study of the influence of metal and ligand nature on the process of thermal decomposition are of a certain interest. This work is a continuation of previously reported studies [15–23] on the thermal and spectral

---

[*] Corresponding author.
E-mail address: uachmoju@savba.sk (S.C. Mojumdar)

0040-6031/00/$ – see front matter © 2000 Elsevier Science B.V. All rights reserved.
PII: S0040-6031(99)00456-6

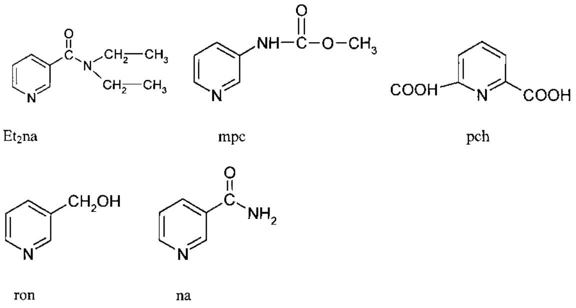

Scheme 1.

properties of Mg(II) complexes with pyridine and substituted pyridines. This paper describes the preparation of complexes formed by the Et$_2$na, na, mpc or ron with pch (see Scheme 1), along with thermal analyses and IR spectral investigation of prepared complexes.

2. Experimental

2.1. Preparation of compounds

The complexes **I–IV** were prepared by treating na, Et$_2$na, mpc or ron (0.01 mol) with Mg(pc)·4H_2O (0.005 mol) in methanol. The solutions were left to stand at room temperature. The fine microcrystals that precipitated were filtered off, washed with diethyl ether and dried at room temperature.

2.2. Measurements

Elemental analyses (C, H, N) were carried out by means of a Carlo Erba 1106 analyzer. The IR spectra were obtained on Philips analytical PU9800 FTIR spectrometer by using Nujol mulls in the range 200–4000 cm^{-1}, while thermal decomposition studies were carried out on Paulik–Paulik–Erdey Derivatograph (Type OD 102, MOM, Budapest) in air atmosphere by using a platinum crucible with a sample weight of 100 mg in the range 20–1000°C. The rate of temperature increase of 10°C min^{-1} was chosen for all measurements.

3. Results and discussion

3.1. Analytical results of compounds

The content of N, C and H was determined by elemental analysis and the content of Mg(II) was established by complexometric titration. The analytical data of the compounds **I–IV** reported in Table 1 shows a good agreement between the experimental and calculated data.

3.2. Thermal decomposition of the compounds

The thermal decomposition data of compounds **I–IV** are collected in Table 2. The complexes **I–IV** are thermally, relatively stable. Thermal decompositions of the compounds are multi-stage processes. The subsequent detachment of the ligands was observed. The final solid product was always identified as MgO.

The TG and DTA curves for Mg(pc)(na)$_2$·2H_2O (**I**) are shown in Fig. 1. The TG curve of that complex indicates that it is thermally stable up to 150°C, when the slow decomposition to MgO begins, as to the final product formed at 710°C. This is followed by two mass loss steps between 150–300 and 300–580°C. Based on this mass loss value (Table 2), these two steps were attributed to the formation of two intermediate decomposition products, i.e., Mg(pc)(na)$_2$ and Mg(pc). The most probable thermal decomposition scheme is

Table 1
Analytical data of compounds

Complex	Theoretical (%)				Experimental (%)			
	C	H	N	Mg	C	H	N	Mg
Mg(pc)(na)$_2$·2H_2O	48.34	4.03	14.84	5.15	48.30	4.02	14.85	5.13
Mg(pc)(Et$_2$na)·3H_2O	53.87	6.15	11.64	4.04	53.82	6.16	11.65	4.03
Mg(pc)(mpc)$_2$·2H_2O	49.05	4.09	13.63	4.73	49.01	4.07	13.61	4.72
Mg(pc)(ron)·2H_2O	46.35	4.16	8.32	7.22	46.29	4.15	8.30	7.21

Table 2
Thermal decomposition data

Complex	DTA results	TG results			
	T_{peaks} (°C)	T_{range} (°C)	Mass loss (%) found (calculated)	Loss	Composition of the residue found (calculated) (%)
$Mg(pc)(na)_2 \cdot 2H_2O$	160 endo	150–300	7.60 (7.63)	$2H_2O$	MgO 8.50 (8.54)
	350 endo	300–580	51.80 (51.79)	2pic	
	650 exo	580–710	Decomposition		
$Mg(pc)(Et_2na)_2 \cdot 3H_2O$	130 endo	115–210	3.00 (2.99)	H_2O	MgO 6.75 (6.70)
	230 endo	210–360	6.00 (5.99)	$2H_2O$	
	400 endo	360–640	59.25 (59.19)	$2Et_2na$	
	690 exo	640–745	Decomposition		
$Mg(pc)_2(mpc)_2 \cdot H_2O$	140 endo	130–205	3.50 (3.50)	H_2O	MgO 7.80 (7.85)
	250 endo	205–450	29.50 (29.62)	mpc	
	470 endo	450–660	29.75 (29.62)	mpc	
	710 exo	660–740	Decomposition		
$Mg(pc)(ron) \cdot 2H_2O$	210 endo	165–350	10.75 (10.70)	$2H_2O$	MgO 12.00 (11.98)
	390 endo	350–660	32.50 (32.42)	ron	
	720 endo	660–780	Decomposition		

$$Mg(pc)(na)_2 \cdot 2H_2O \overset{150-300^\circ C}{\rightarrow} Mg(pc)(na)_2$$

$$Mg(pc)(na)_2 \overset{300-580^\circ C}{\rightarrow} Mg(pc)$$

$$Mg(pc) \overset{580-710^\circ C}{\rightarrow} MgO$$

The DTA curve for complex **I** (Fig. 1) displays two endothermic peaks maximized at 160 and 350°C corresponding to the loss of $2H_2O$ and 2na, respectively, and an exothermic peak maximized at 650°C corresponding to decomposition reaction involving the loss of pc with simultaneous formation of MgO.

The TG and DTA curves for $Mg(pc)(Et_2na)_2 \cdot 3H_2O$ (**II**) are shown in Fig. 2. The TG curve for that complex indicates that it is thermally stable up to 115°C, when the slow decomposition to MgO begins, as to the final product formed at 745°C. This is followed by three mass loss steps between 115–210, 210–360 and 360–640°C. Based on this mass loss value (Table 2), these three steps were attributed to the formation of three intermediate decomposition products, i.e., $Mg(pc)(Et_2na)_2 \cdot 2H_2O$, $Mg(pc)(Et_2na)_2$ and

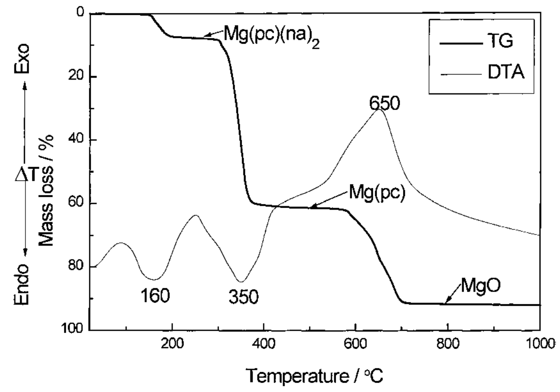

Fig. 1. TG and DTA curves of $Mg(pc)(na)_2 \cdot 2H_2O$ (**I**).

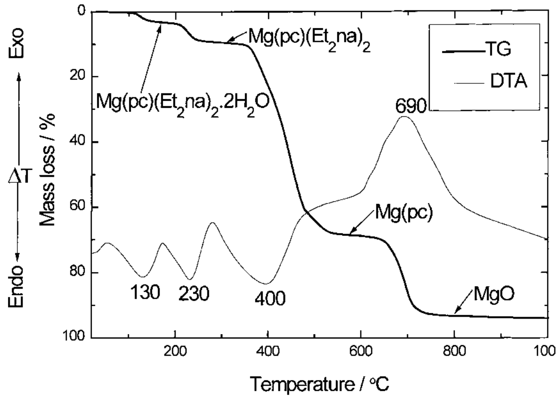

Fig. 2. TG and DTA curves of $Mg(pc)(Et_2na)_2 \cdot 3H_2O$ (**II**).

Mg(pc). The most probable thermal decomposition scheme is

$$\mathrm{Mg(pc)(Et_2na)_2\cdot 3H_2O} \xrightarrow{115-210^\circ\mathrm{C}} \mathrm{Mg(pc)(Et_2na)_2\cdot 2H_2O}$$

$$\mathrm{Mg(pc)(Et_2na)_2\cdot 2H_2O} \xrightarrow{210-360^\circ\mathrm{C}} \mathrm{Mg(pc)(Et_2na)_2}$$

$$\mathrm{Mg(pc)(Et_2na)_2} \xrightarrow{360-640^\circ\mathrm{C}} \mathrm{Mg(pc)}$$

$$\mathrm{Mg(pc)} \xrightarrow{640-745^\circ\mathrm{C}} \mathrm{MgO}$$

The DTA curve for complex **II** (Fig. 2) presents three endothermic peaks maximized at 130, 230 and 400°C corresponding to the loss of H_2O, $2H_2O$ and Et_2na, respectively, and an exothermic peak maximized at 690°C corresponding to decomposition reaction involving the loss of pc with simultaneous formation of MgO.

The TG and DTA curves for $\mathrm{Mg(pc)(mpc)_2\cdot H_2O}$ (**III**) are shown in Fig. 3. The TG curve for that complex indicates that it is thermally stable up to 130°C, where the dehydration process commences. This is followed by three mass loss steps between 130–205, 205–450 and 450–660°C. Based on this mass loss value (Table 2), these three steps were attributed to the formation of three intermediate decomposition products, i.e., $\mathrm{Mg(pc)(mpc)_2}$, Mg(pc)(mpc) and Mg(pc), while the final solid product is concluded to be MgO. The most probable thermal decomposition scheme is

$$\mathrm{Mg(pc)(mpc)_2\cdot H_2O} \xrightarrow{130-205^\circ\mathrm{C}} \mathrm{Mg(pc)(mpc)_2}$$

$$\mathrm{Mg(pc)(mpc)_2} \xrightarrow{205-450^\circ\mathrm{C}} \mathrm{Mg(pc)(mpc)}$$

$$\mathrm{Mg(pc)(mpc)} \xrightarrow{450-660^\circ\mathrm{C}} \mathrm{Mg(pc)}$$

$$\mathrm{Mg(pc)} \xrightarrow{660-740^\circ\mathrm{C}} \mathrm{MgO}$$

The DTA curve for complex **III** (Fig. 3) displays three endothermic peaks maximized at 140, 250 and 470°C corresponding to the loss of H_2O, mpc and mpc, respectively, and an exothermic peak maximized at 710°C corresponding to decomposition reaction involving the loss of pc with simultaneous formation of MgO.

The TG and DTA curves for $\mathrm{Mg(pc)(ron)\cdot 2H_2O}$ (**IV**) are shown in Fig. 4. The TG curve of that complex indicates that it is thermally stable up to 165°C, where the dehydration process commences. This is followed by two mass loss steps between 165–350 and 350–660°C. Based on this mass loss value (Table 2), these two steps were attributed to the formation of two intermediate decomposition products, i.e., Mg(pc)(ron) and Mg(pc), while the final solid product is concluded to be MgO. The most probable thermal decomposition scheme is

$$\mathrm{Mg(pc)(ron)\cdot 2H_2O} \xrightarrow{165-350^\circ\mathrm{C}} \mathrm{Mg(pc)(ron)}$$

$$\mathrm{Mg(pc)(ron)} \xrightarrow{350-660^\circ\mathrm{C}} \mathrm{Mg(pc)}$$

$$\mathrm{Mg(pc)} \xrightarrow{660-780^\circ\mathrm{C}} \mathrm{MgO}$$

The DTA curve for complex **IV** (Fig. 4) displays two endothermic peaks maximized at 210 and 390°C corresponding to the loss of $2H_2O$ and ron, respectively, and an exothermic peak maximized at 720°C corresponding to decomposition reaction

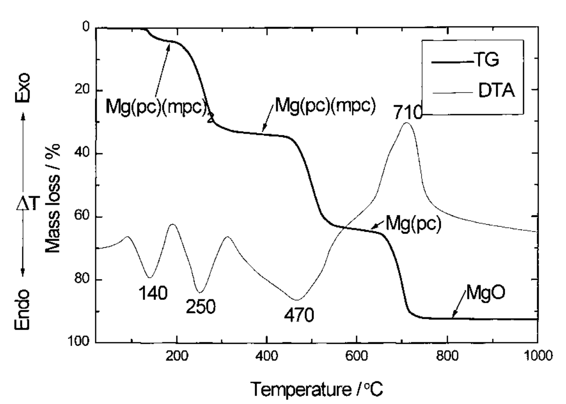

Fig. 3. TG and DTA curves of $\mathrm{Mg(pc)(mpc)_2\cdot H_2O}$ (**III**).

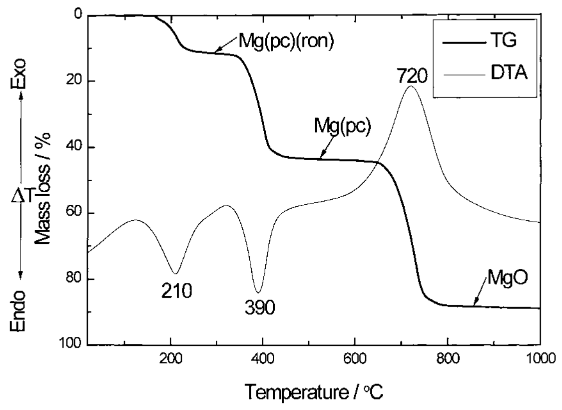

Fig. 4. TG and DTA curves of $\mathrm{Mg(pc)(ron)\cdot 2H_2O}$ (**IV**).

Table 3
IR spectral data (4000–200 cm^{-1}) of complexes **I**–**IV** (as=antisymmetric and s=symmetric)

Assignments	**I**	**II**	**III**	**IV**
$\nu_{(\mathrm{CO})}$	1665	1654	1669	–
$\nu_{(\mathrm{CN})}$	1607	1608	1605	1606
$\gamma_{(\mathrm{CCC})}$	668	688	681	672
	612	611	610	613
Mg–N	216 224, 239	213 228, 239	216 233, 242	206 225, 238
$\nu_{\mathrm{COO^-(as)}}$	1698	1699	1696	1693
$\nu_{\mathrm{COO^-(s)}}$	1423	1406	1407	1410
Δ_{COO}	275	293	289	283
$\nu_{(\mathrm{C-C})}$	971	972	974	975
$\nu_{(\mathrm{C-H})_{\mathrm{ac}}}$	2845 916	2847 919	2846 921	2848 922
$\nu_{(\mathrm{C-H})_{\mathrm{ring}}}$	861	862	863	864
$\nu_{(\mathrm{OH})}$	3345	3249 3356	3318	3385
$\delta_{(\mathrm{HOH})}$	1615	1613	1614	1611
Others (650–1000 cm^{-1})	724 751, 762	747 762, 780	654 760, 833	742 760, 804
	778 800, 920	854 950	857 890, 941	833 841, 941
$\nu_{(\mathrm{Mg-O})}$	252 372, 390	250 271, 305	303 380	302 363
$\pi_{(\mathrm{CO_2})}$	539	540	538	541

involving the loss of pc with simultaneous formation of MgO.

3.3. IR spectra

The modes of the coordinated ligands in the complexes have been investigated by means of IR absorption spectra. The most important IR frequencies attributed to the vibrations of the complexes **I**–**IV** are reported in Table 3. The IR spectra of complexes **I**–**IV** show broad absorption bands in the range 3249–3385 cm^{-1}. These frequencies of complexes **I**–**IV** correspond to the antisymmetric and symmetric OH stretch [24,26]. These bands clearly confirm the presence of water in complexes **I**–**IV**. The compounds showed the carboxylate stretching frequencies, $\nu_{\mathrm{COO^-(s)}}$ in the range 1406–1423 cm^{-1} and $\nu_{\mathrm{COO^-(as)}}$ in the range 1693–1699 cm^{-1}. The position of the bands are characteristic of metal(II) carboxylate compounds [25]. Carboxylate ions can coordinate to metal ions in a number of ways such as unidentate, bidentate (chelating) or bridging and there is an evidence of that fact in the IR spectrum. The analysis of COO$^-$ group bands frequencies allowed on the determination of the parameter $\Delta_{\mathrm{COO}} = \nu_{\mathrm{COO^-(as)}} - \nu_{\mathrm{COO^-(s)}}$. The magnitude of Δ_{COO} has been used by Nakamoto [26] as a criteria of the way of carboxylate binding with metal ions. Calculated from the examined spectra values of Δ_{COO} are in the range 293–275 cm^{-1}. These values and three bands (COO deformation) at 920–720 cm^{-1} of complexes **I**–**IV** is in good accord with the literature data for unidentately bonded acetates structures. The stretching vibration of the C=N in the pyridine ring appeared at 1590 cm^{-1} [27]. Upon complex formation the peak shifts to higher frequencies [28]. The shifts in complexes **I**–**IV** (in the range 1605–1608 cm^{-1}) may suggest that the bond formation of the metal with the N of pyridine ring increases the dipolar contribution of C=N$^+$ in the heterocyclic ring [27]. The absorption bands which occur in the range 242–206 cm^{-1} $\nu_{(\mathrm{Mg-N})}$ also confirm the coordination of na, Et$_2$na, mpc and ron to Mg(II) through the nitrogen atom of respective heterocyclic ring.

4. Conclusions

All of the complexes **I**–**IV** are hydrated, stable in air and soluble in water, ethanol, methanol and dimethylsulfoxide. In complexes **I**, **II** and **IV** loss of the neutral ligands occurs (on the TG curves) in one step and in complex **III** in two steps. The thermal stability of the complexes can be ordered in the sequence: **II**<**III**<**I**<**IV**. The results reveal that MgO is left as residue at the end of the thermal degradation experiments of the compounds **I–IV**. The stoichiometry of thermal decomposition can also be influenced by the changes of experimental conditions [29,30]. IR data is in good accord with the literature data for unidentately bonded acetates structures. Et_2na, na, mpc and ron were coordinated to Mg(II) through the nitrogen atom of the respective heterocyclic ring in complexes **I–IV**. The preliminary study has shown that the complexes do have a biological activity. Without X-ray analysis, no definite structure can be described for the different components. However, spectroscopic and analytical data available enable us to predict structures and we can also use thermal decomposition studies to help us.

Acknowledgements

The authors wish to thank the Ministry of Education of the Slovak Republic for financial support.

References

[1] E. Jóna, M. Kubranová, P. Šimon, J. Mroziński, J. Thermal Anal. 46 (1996) 1325.
[2] E. Jóna, A. Sirota, P. Šimon, M. Kubranová, Thermochim. Acta 258 (1995) 161.
[3] B. Papánková, A. Mašlejová, P. Šimon, TERMANAL 97, in: Proceedings of the International Conference on Belusské Slatiny, Slovakia, 1–3 October 1997, CHTF-STU Press, Bratislava, 1997.
[4] J.S. Skoršepa, K. Györyová, M. Melník, J. Thermal Anal. 44 (1995) 169.
[5] K. Györyová, F.A. Nour El-Dien, TERMANAL 97, in: Proceedings of the International Conference on Belusské Slatiny, Slovakia, 1–3 October 1997, CHTF-STU Press, Bratislava, 1997.
[6] E. Jóna, M. Hvastijová, J. Kohout, J. Thermal Anal. 41 (1994) 161.
[7] W. Linert, M. Enamullah, V. Gutmann, R.F. Jameson, Monatsh. Chem. 125 (1994) 661.
[8] K. Kundu, M.A.H. Miah, Jahangirnagar Univ. J. Sci. 19 (1995) 49.
[9] M. Enamullah, W. Linert, J. Coord. Chem. 35 (1995) 325.
[10] G. D'ascenzo, U.B. Ceipidor, E. Cardarelli, A.D. Magri, Thermochim. Acta 13 (1975) 449.
[11] M. Melník, L. Macášková, J. Mroziński, Polyhedron 7 (1988) 1745.
[12] M. Melník, I. Potočnak, L. Macášková, D. Mikloš, Polyhedron 15 (1996) 2159.
[13] E. Jóna, M. Jamnický, J. Thermal Anal. 27 (1983) 359.
[14] M. Melník, M. Koman, T. Glowiak, Polyhedron 17 (1998) 1767.
[15] S.C. Mojumdar, M. Melník, E. Jóna, Polish J. Chem. 73 (1999) 293.
[16] S.C. Mojumdar, M. Valko, M. Melník, Chem. Papers 52 (1998) 650.
[17] S.C. Mojumdar, M. Melník, E. Jóna, J. Anal. Appl. Pyrol. 46 (1998) 147.
[18] S.C. Mojumdar, M. Melník, M. Valko, Polish J. Chem. 73 (1999) 457.
[19] S.C. Mojumdar, M. Melník, E. Jóna, J. Anal. Appl. Pyrol. 48 (1999) 111.
[20] S.C. Mojumdar, D. Hudecová, M. Melník, Polish J. Chem. 73 (1999) 759.
[21] S.C. Mojumdar, M. Melník, E. Jóna, J. Thermal Anal. Cal. 56 (1999) 533.
[22] S.C. Mojumdar, M. Melník, E. Jóna, J. Thermal Anal. Cal. 56 (1999) 541.
[23] S.C. Mojumdar, M. Melník, E. Jóna, D. Hudecová, Chem. Papers 53 (1999) 265.
[24] G. Deveto, G. Ponticelli, C. Preti, J. Inorg. Nucl. Chem. 37 (1975) 1635.
[25] K. Nakamoto, Y. Morimoto, A.E. Martell, J. Am. Chem. Soc. 83 (1961) 4528.
[26] K. Nakamoto, Infrared and Raman Spectra of Inorganic and Coordination Compounds, 4th Edition, Wiley, New York, 1986.
[27] D. Aslanian, A. Lautic, Ch. Mantai, M. Baltanski, J. Chim. Phys. 72 (1957) 1052.
[28] Y. Kidani, M. Noji, H. Koike, Bull. Chem. Soc. Jpn. 48 (1975) 239.
[29] T. Šramko, G. Liptay, E. Jóna, J. Thermal Anal. 12 (1977) 217.
[30] Y. Masuda, Thermochim. Acta 39 (1980) 235.